OPEN JOURNAL SYSTEMS
ISSN:2237-2202

Available on line at Directory of Open Access Journals

Journal of Hyperspectral Remote Sensing v.6, n.4 (2016) 184-194
DOI: 10.5935/2237-2202.20160019

Journal of Hyperspectral Remote Sensing
www.ufpe.br/jhrs

Surface temperature in response to changes in coverage and due to land use urban expansion: a study in Brasilia-DF

Lidiane C. F. Gomes[*], Carlos A. C. dos Santos[**], Bernardo B. da Silva[***], Bergson G. Bezerra[****], Felipe F. Monteiro[*****]

*PhD professor Federal Institute of Education, Science and Technology of Paraíba – IFPB, R. Antônio dos Santos, s/n. Centro, Picuí – PB - Brasil. Email: lidiane.geo@gmail.com (Corresponding author)
**PhD professor at the Federal University of Campina Grande - UFCG, Department of Atmospheric Sciences/UACA.
***PhD professor at the Federal University of Campina Grande - UFCG, Department of Atmospheric Sciences/UACA.
****PhD professor at the Federal University of Rio Grande do Norte - UFRN, Center of Exact Sciences and Earth/CCET.
*****Doctoral candidate in Climate Science; Federal University of Rio Grande do Norte - UFRN.

Received 28 January 2016; accepted 20 April 2016

Abstract

The objective of this study was to evaluate the dynamics of temperature of the land surface and land use through TM-Landsat 5 images, between 1987 and 2011 in Metropolitan Brasilia, the Federal District. The city was chosen to present quite peculiar characteristics resulting from its urban planning, including as regards its location, and that over the years has been modified due to the new trends in occupation of its territory. Satellite images were used Landsat 5-TM and SEBAL. The results indicated that the expansion of urban areas has contributed to a significant increase in temperatures over the years, but in the Pilot Plan, it was revealed that there was a cooling mostly derived from the implementation of wooded medians. In impermeable areas, the temperatures approached 30°C and was verified environments conducive to formation of urban heat islands.

Keywords: Remote sensing, land use, urban climate , urban heat islands.

1. Introduction

The population dynamics of rural Brazil has been marked in the last 50 years by the drastic decrease in its population (Foehlich et al., 2011) due to the rural exodus that has remained fairly sharp until the mid-90 As a result, there was increased concentration of people in urban areas, which derived an accelerated urban expansion of large Brazilian cities, in most cases in a disorderly manner and without any planning. The accelerated urban expansion process that provides a sharp change of land cover, usually replacing a natural environment for building, asphalt, etc., is mainly due the significant increase in the surface temperature (Ts), leading to a microclimate condition It is substantially hotter than the surrounding non-urbanized areas (Oke, 1973; Voogt and Oke, 2007; Gartland, 2010; Menberg et al., 2013.). According Koenigsberger et al. (1980) in those areas the temperature may be increased by up to 8 ° C and the relative humidity of air reduced 5 to 10% due paving which provides fast evaporation of water and lack of vegetation.

This phenomenon gives the name of Urban Heat Islands (UHI) and occur primarily due to the heat radiation of differences between built-up areas and regions that preserve natural features. During the day, the buildings serve as reflection of mazes in the higher layers of heated air also prevents air circulation. At night, the air pollution prevents heat dispersion (Lombardo, 1985). This microclimate condition causes

significant effects on human health (Patz et al., 2005), worsening of local pollution (Lo and Quattrochi, 2003), impairment of pollutant dispersion process (Serrat et al., 2006; Ram et al, 2007; Clinton and Gong, 2013) and wider impacts on the climate at the regional scale (Yang et al., 2011; Clinton and Gong, 2013).

The Ts is of paramount importance for the study of urban climatology, because it modulates the air temperature of the lower layers of the urban atmosphere, the energy balance at the surface and affects the energy changes that interfere with the comfort of city dwellers (Voogt and Oke, 2007). In this context, remote sensing has been an important tool in UHI detection (Yuan and Bauer, 2007; Pichieri et al, 2012; This et al., 2012; Clinton and Gong, 2013).

This detection is usually made from Ts analysis, which in turn is estimated based on the radiance of the thermal band satellite sensors such as the TM (Thematic Mapper) and ETM + (Enhanced Thematic Mapper Plus), both on board the satellite Landsat (Stathopoulo and Cartalis, 2007; Yuan and Bauer, 2007; This et al., 2012;. Lazzarini et al., 2013), MODIS (Moderate Resolution Imaging Spectroradiometer) aboard the Terra and Aqua satellites (Pichieri et al., 2012; Clinton and Gong, 2013) and AVHRR (Advanced Very High Resolution Radiometer) onboard the NOAA (Streutker, 2003).

The advantage of remote sensing use in this type of study is that it provides estimates of Ts spatialized, allowing the simultaneous analysis of the behavior of the same in areas with ground cover dynamic differentiated in the same scene, which facilitates the identification of any UHI.

For such use, it was chosen SEBAL (Surface Energy Balance Algorithm for Land), whose mathematical formulas are able to extract various analyzes of the Earth's surface. The SEBAL has widespread use with respect to obtaining the evapotranspiration and compose a set of steps, offers a range of products, which can also be used in environmental studies and urban climate, is to quantify the vegetation, obtaining surface temperature and radiation balance, such as Delgado et al., (2012).

Given the above, this study aims to evaluate the dynamics of Ts and land use through TM-Landsat 5 images, and GIS techniques, between 1987 and 2011 in Metropolitan Brasilia, the Federal District, which have characteristics quite peculiar resulting from its urban planning, including as regards its location, and that over the years has been modified with the appropriation of new trends in occupation of their territorial space, such as the vertical.

2. Materials and methods

The study area comprises a cutout in the metropolitan region of Brasília-DF located in the Central Plateau of Brazil, between the geographic coordinates: latitude 15 ° 42 'S and longitude 47 ° 57' W. It has a population of about 2,562,963 inhabitants (IBGE, 2011). It is characterized by tropical climate, according to Köppen classification, which are identified two distinct seasons: hot and wet (October to April) and dry (May to September). Its climate is characterized by high temperature range. In the colder months (June and July), the minimum temperatures are below 18 ° C, while in the warmer months (September and October) the maximum temperature can exceed 30 °C (Maciel, 2002).

To carry out this study, images from Landsat 5 satellite - TM, orbit 221, paragraph 71, the dates of 06/07/1987 and 25/08/2011. The spectral bands used were treated by intra and inter mathematical procedures bands, orthorectification, clippings, and operations depending on the specificities of each. Mathematical operations were carried out from SEBAL - Surface Energy Balance Algorithms for Land, as shown in Figure 1.

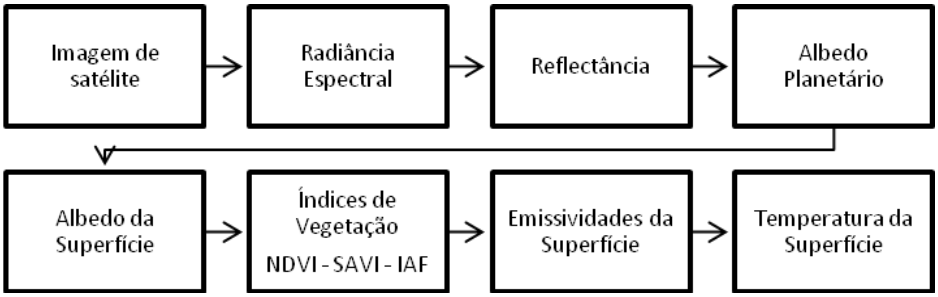

Figure 1 – Flow chart of the computational steps for obtaining the surface temperature (Ts) through SEBAL.

To calculate the spectral radiance of each band (Lλi) was used the equation proposed by Markham and Baker (1987), and the realization of radiometric calibration converting the digital number (ND) of each pixel of the image in monochrome spectral radiance.

$$L_{\lambda i} = a_i + \frac{b_i - a_i}{255} ND \quad (1)$$

They are: a_i and b_i the minimum and maximum spectral radiance, respectively, in W m-2 sr-1 μm-1, 255 is the maximum number of gray levels or radiometric resolution of TM sensor; i corresponds to bands 1 to 7 TM sensor on board the satellite Landsat 5. The monochrome reflectance of each band (ρλi) is the ratio between the radiant flux reflected by a surface and the incident. The calculation was made using the equation proposed by Allen et al. (2002).

$$\rho_{\lambda i} = \frac{\pi L_{\lambda i}}{K_{\lambda i}.\cos Z.d_r} \quad (2)$$

Where: $K_{\lambda i}$ a solar spectral irradiance of each band at the top of the atmosphere (W m-2 uM-1), Z is the solar zenith angle in radians; dr is the square of the ratio of the average Earth-Sun distance is calculated using the formula quoted by Iqbal (1983):

$$d_r = 1 + 0{,}033.\cos\left(\frac{DSA.2\pi}{365}\right) \quad (3)$$

Wherein the argument of the cosine function is measured in radians. The average annual value of dr varies between 0.97 and 1.03.

The DSA corresponds to the sequence of the year. In area with very small or no slope, the cosine of the incidence angle of the solar radiation is simply obtained from the Sun elevation angle (E), which is in the picture header at the time of purchase, using equation 4.

$$\cos Z = \cos\left(\frac{\pi}{2} - E\right) \quad (4)$$

The next step consisted of getting the vegetation indices such as the NDVI (Normalized diference Vegetation Index) that according to Ponzoni and Shimabukuro (2009) has been widely used and exploited in different approaches in agricultural research, forestry and climate. The NDVI is obtained by the ratio between the difference of the reflectances of near infrared bands (ρIV) and red (ρIV) and the sum of them, according to the following equation:

$$NDVI = \frac{\rho_{IV} - \rho_V}{\rho_{IV} + \rho_V} \quad (5)$$

The SAVI (Soil Adjusted Vegetation Index) is a vegetation index proposed by Huete (1988) that seeks to offset the effects of the "background" of the soil, which is calculated by the following equation:

$$SAVI = \frac{(1 + L)\rho_{IV} - \rho_V}{(L + \rho_{IV} + \rho_V)} \quad (6)$$

Wherein L is a factor used a soil function. Some studies using L = 0.1, although its value is most widely used L = 0.5 (Huete and Warrick, 1990; Accioly et al, 2002;. Boegh et al., 2002). This study used L = 0.5. Then we calculated the LAI (Leaf Area Index) which is an indicator of biomass of each pixel of the image. It is defined as the ratio between the leaf area of all vegetation per unit area used by this vegetation.

$$IAF = \frac{\ln\left(\frac{0{,}69 - SAVI}{0{,}59}\right)}{0{,}91} \quad (7)$$

To obtain Ts, it is necessary to obtain the emissivity of each pixel in the spectral domain of the thermal band Landsat TM 5 (10.4 - 12.5 μm), the εNB, which can be obtained by expression input by Allen et al. (2002).

$$\varepsilon_{NB} = 0{,}97 + 0{,}00331 \times IAF \quad (8)$$

The emissivity can be obtained for NDVI> 0 and IAF> 3, but for cases with the IAF ≥ 3, the $\varepsilon_{NB} = \varepsilon_0 = 0{,}98$ and bodies water, NDVI <0, , $\varepsilon_{NB} = 0{,}99$ and $\varepsilon_0 = 0{,}985$, recommended by Allen et al. (2002). Finally, Ts (K) was calculated by reversed Planck equation as Markham and Barker (1987), based on the spectral radiance of the termal band Lλ,6 e εNB.

$$Ts = \frac{K_2}{\ln\left(\frac{\varepsilon_{NB} K_1}{L_{\lambda,6}} + 1\right)} \quad (09)$$

Where K1 = 607.76 W m-2 uM-1 sr-1 and K2 = 1260.76 K are constant calibration of the thermal band of Landsat 5 - TM. From a color composition 234 BRG, for the years 1987 and 2011, in order to evaluate changes in land cover and verify its relation to the surface temperature of the dynamics in the region. A supervised classification using the calculator Maxver was held, where from the visual analysis of the images were defined 5 classes for the study: Urban Area, Water, Soil exposed, dense vegetation and small vegetation.

With this definition samples were collected for each class, the samples have undergone a process of statistical analysis performed by the software itself, to check the accuracy of the collected samples. After this stage the process was the proper classification, where it outputs the classified image, which then underwent a post-assessment, which refined the results found in the classification image and the end mapping classes, which transforms final image in thematic category, allowing extract the classified image measurement of each class identified in the image.

The surface temperature analysis occurred in two stages, the first allowed an overview of the study area, the second stage highlighted six (06) representative points, distributed in the metropolitan area of Brasilia and surrounding urban centers, noting the association of temperatures ground to their respective compositions.

The effect of urbanization was also assessed by Waterproof Surface Area (ISA, term Impervious Surface Area), which represents the fraction of the surface in which there is infiltration of rainwater and / or evaporation of soil moisture (Carlson and Arthur, 2000. Gutierrez et al, 2011).. ISA was calculated by the following equation, according to Carlson and Arthur (2000):

$$ISA = \left[1 - \left(\frac{NDVI - NDVI_0}{NDVI_S - NDVI_0}\right)^2\right]_{dev} \quad (10)$$

Where NDVIS indicates the values for dense vegetation, NDVI 0 represents the values for bare soil and the index dev indicates that the formula should be used only to areas classified as urban. In this study was used for the year 1987 NDVIS = 0.65 and = 0.09 NDVI0 and for the year 2011, the NDVI S = 0.60 and NDVI 0 = 0.07, both extracted from the used images for the respective years. ISA ranges from 0 to 1, with values closer to 1 indicate more impervious areas, while the next values of 0 indicate areas with permeable surface (and Arthur Carlson, 2000).

3. Results and discussion

Figure 2 presents the results obtained by the supervised classification, it is observed that the urban area grew significantly in parts of northeast and southeast of the study area. It was also smooth urbanization of expression in the northern part. In class "Dense vegetation" there was an increase of 24.6%, as shown in Table 1 and can be viewed in the northwestern part of Figure 2b.

Quantitatively evaluating the ratings realize that there was a reduction in bare soil class 47.8%, giving rise to new urbanized areas and the small vegetation that grew about 0.2%. Can be viewed in the region called North Wing of the urban design of the city of Brasilia, Figure 2a, where there were large concentrations of urban areas and bare soil and that over the years have become vegetated areas, derived from urban proposals with beds vegetation. In the South Wing it was also the appearance of areas with small vegetation, possibly associated with the growth of the housing area.

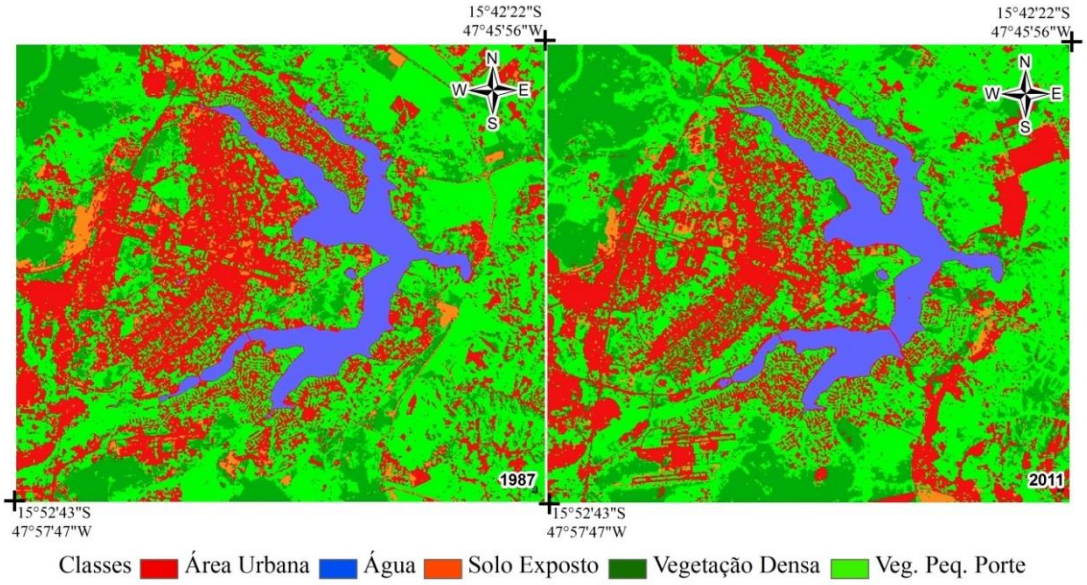

Figure 2 – Map of use and occupation of the years 1987 (a) and 2011 (b).

In addition to the spatial distribution of targets observed in Figure 2, the measurement of the total area of each class was extracted, as shown in Table 1, which can be confirmed changes in space, due to urbanization and local way of life. One can observe the column labeled "difference" that shows the dynamics of land cover in the five (05) classes identified for the period of 24 years.

Table 1 - Thematic classes derived from maps of land use and occupation in the years 1987-2011 for Brasilia-DF.

Thematic classes	Areas - ha		Differences (ha)	Differences (%)
	1987	2011		
Urban Area	16099,4	15123,8	-976,1	-6,1
Water	3574,3	3469,9	-104,4	-2,9
Exposed Soil	1376,3	718,8	-657,5	-47,8
Dense Vegetation	6859,1	8547,8	1688,7	24,6
Small Porte Vegetation	20856,1	20905,4	49,3	0,2

The urban area decreased by 6.1% as a whole, which may have resulted from a process of change pavements, parks or insertion resulting from a spectral mixture of assessed targets. The bare soil class, also had a reduction of area which can be associated with the expansion of ground cover by vegetation of grassy type or another type of vegetation that includes the Cerrado, present in the region.

The water class was detected a decrease of 2.9% which can be attributed to the absence of bodies of water or intermittent change in the local water system, as well as changes in physical and chemical composition of water, landfill or siltation of aqueous regions or even same spectral mixture of targets at the time of rating derived from damp soil, for example.

In addition to the spatial distribution of targets observed in Figure 2, the measurement of the total area of each class was extracted, as shown in Table 1, which can be confirmed changes in space, due to urbanization and local way of life. One can observe the column labeled "difference" that shows the dynamics of land cover in the five (05) classes identified for the period of 24 years.

The urban area decreased by 6.1% as a whole, which may have resulted from a process of change pavements, parks or insertion resulting from a spectral mixture of assessed targets. The bare soil class, also had a reduction of area which can be associated with the expansion of ground cover by vegetation of grassy type or another type of vegetation that includes the Cerrado, present in the region.

The water class was detected a decrease of 2.9% which can be attributed to the absence of

bodies of water or intermittent change in the local water system, as well as changes in physical and chemical composition of water, landfill or siltation of aqueous regions or even same spectral mixture of targets at the time of rating derived from damp soil, for example.

The spatial distribution of surface albedo (Figure 3), the color scale grayscale comprises the albedo values between 0 to 0.35 with average values of 0.18. Depending on their texture, color and chemical composition, small vegetation, dense, water and bare ground showed values close to 0.14, 0.09, 0.03 and 0.20, respectively. In urban areas, depending on their use and occupation, presented distinct values; asphalt values around 0.11, concrete and clearer coverage, values between 0.26 to 0.35.

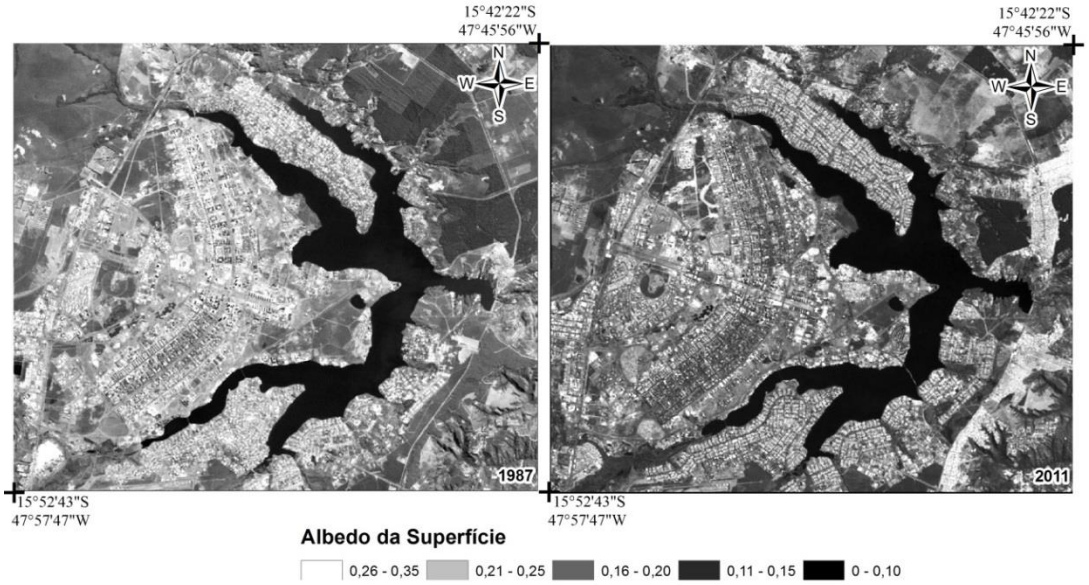

Figure 3 – Spatial distribution of surface albedo between the years 1987 (a) and 2011 (b).

Within the urban area (Figure 3a) there is greater reflectivity of targets, ground-based exposed and buildings covers with light colors. In Figure 3b, it is noted that the pilot level shows a decrease of the albedo of the soil derived from the occupation by dark coloring materials such as asphalt pavement.

Already in the eastern and southeastern parts of the study area there has been a considerable increase in the albedo derived from the expansion of urban areas with buildings using metal roofing, as well as the emergence of bare soil. Figure 4 shows the spatial distribution of NDVI, with values ranging from -1.0 to 0.77, in which its maximum value corresponds to the least dense vegetation and to water bodies.

Also in Figure 4, you may notice a decrease in their values and aspects between the years 2011 and 1987 and can be seen in greater representation, the loss of vegetation in the northeast (Figure 4a), which changes due to agricultural activities.

In the central part there was better representation of its values in the North and South wing and kept its characteristics in the areas of riparian forests in this area of study. In the southeastern part can be seen the removal of vegetation and, as shown in Figure 4b, this region was replaced by urban area.

The values of Impermeable Surface Area (ISA) shown in Figure 5 between 0 and 1, wherein 0 to 0,20 range comprises more permeable regions as healthy vegetation planting areas and gallery forest.

Areas with dense vegetation present the treetops as a barrier, inhibiting the direct infiltration into the soil and are present in class values between 0,21 to 0,60.

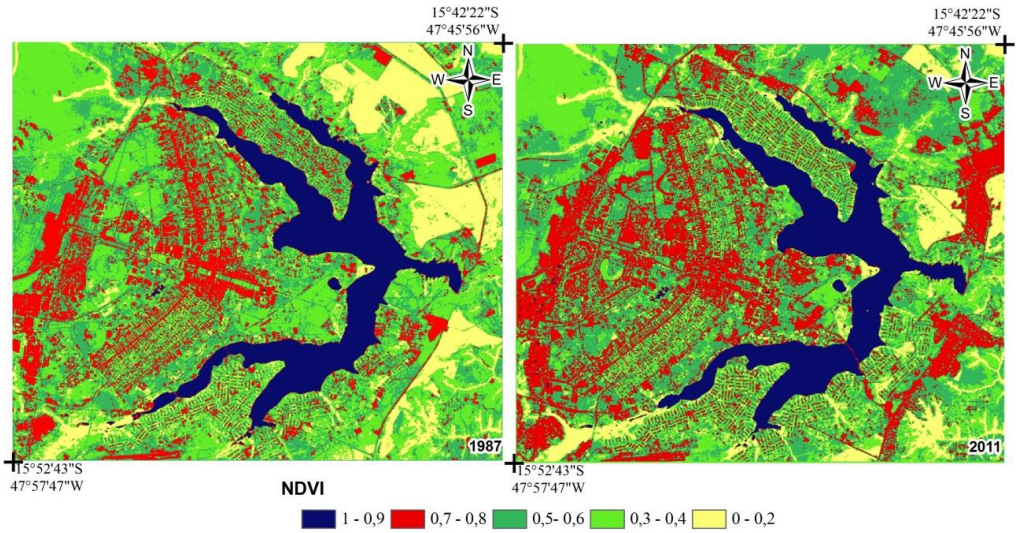

Figure 4 – Spatial Distribution of Vegetation Index (NDVI) between the years 1987 (a) and 2011 (b).

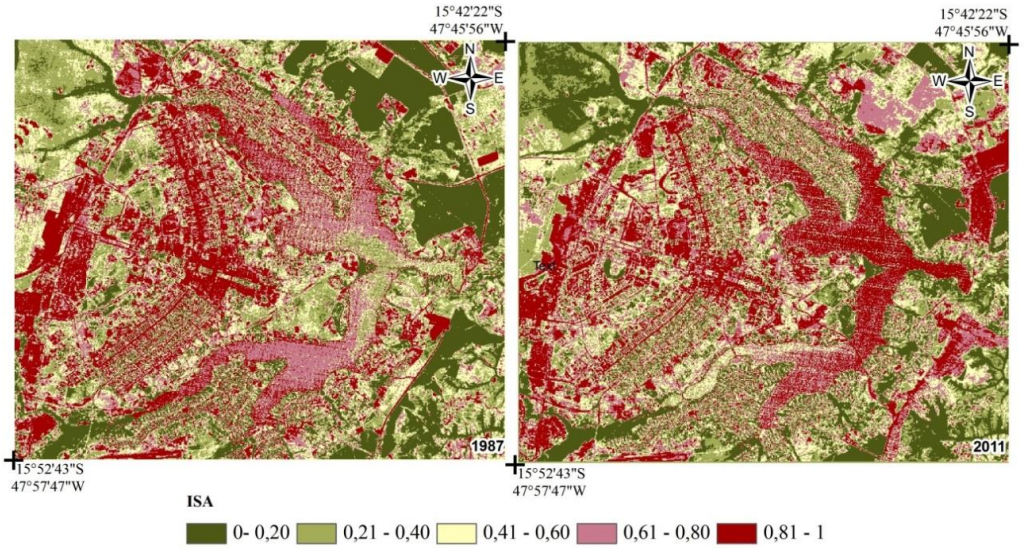

Figure 5 – Spatial distribution of Waterproof Surface Area (ISA) between the years 1987 (a) and 2011 (b).

In urban areas there was an increase in intensity of dark tones over the years, with values close to 1, especially in the northeast and southeast areas of Figure 5b, due to the presence of new urban areas. On the roads master plan can be observed well delineated, but its greatest intensity can be seen in Figure 5b, referring to urbanized areas.

As historical evolution of surface albedo parameters (Figure 3), the vegetation cover (Figure 4), ISA (Figure 5) and the use and land cover map (Figure 2), there were also changes in temperature charts (Figure 6) between the years 1987 and 2011.

In 1987 (Figure 6a) in the region of North Wing, temperatures can be observed from 14 to 18 ° C in concentrated areas and other locations where they are indicated as urban areas. Warmer temperatures, as expected, can be checked where there are water bodies and vegetated areas.

The spatial distribution of the 2011 year of temperature (Figure 6b) showed legend colors with higher values where the maximum indicated a change around 12 ºC and a minimum of about 2 °C. In the master plan, the North and South Wings showed mild temperatures due to the implementation of vegetated sites, areas with higher temperature are distributed spatially across the image (Figure 6b), derived from urban growth, with the removal of vegetation cover, waterproofing of various roads and construction materials with high thermal capacity.

In order to evaluate the surface temperature over the use and land cover were

chosen four strategic points within the study area, as shown in Figures 7 to 10. The first point chosen is located in the North Wing Pilot Plan (Figure 7), which it is an incorporated area of a shopping center, containing a shopping mall, large enterprise and an education center.

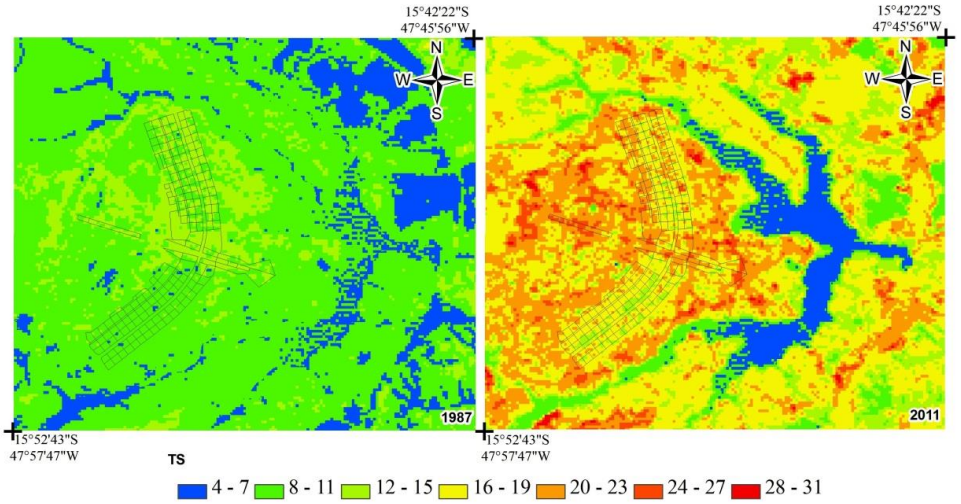

Figure 6 – Spatial distribution of surface temperature (TS) between the years 1987 (a) and 2011 (b).

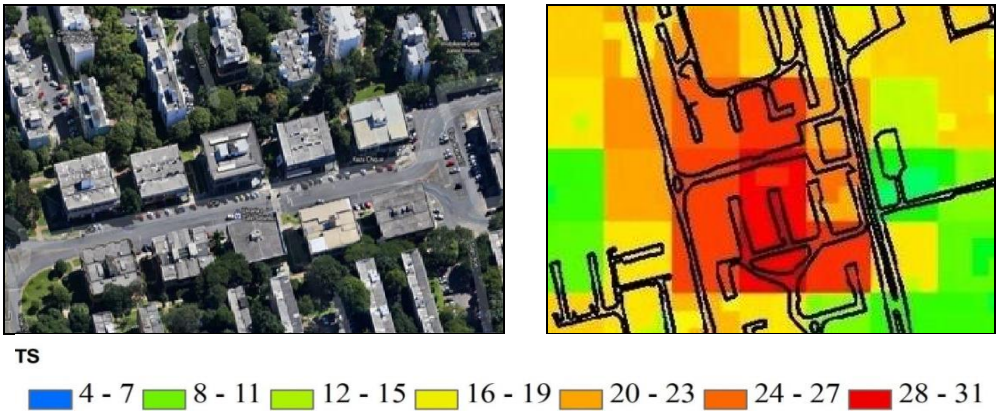

Figure 7 – Spatial distribution of surface temperature in the North Wing Pilot Plan (Point 1), for the year 2011.

Analysing the Figure 7, it is noted that the paved urban roads with bituminous material and roofs of buildings mostly asbestos material showed near 30 °C temperature, contrasting with the surrounding vegetated areas where temperatures ranged from about 12 ºC to about 20 ºC . The temperature difference between the surrounding area and the central area of the image exceeds 10 °C, that the presence of large internal temperature contrasts according Gartland (2010) are indicative of that mark the presence of islands of heat.

The areas with high temperatures are derived impermeable areas, wherein as surface albedo absorbs a greater amount of electromagnetic radiation (EMR), and consequently most of the heating surface. The areas with vegetation presence at the site to dry the tendency of smoothing of surface temperatures, since the vegetation on the presents of REM are driven through their stomata, contained in the leaves, to release to the atmosphere water under vapor form.

Figure 8 is the Point 2 located between the North and South Wings, in a large urban road, near the Plaza of retirees. According to the temperature map shown in Figure 8 the most heated region is the center of the avenue, thick asphalt. Like the previous point there is differences of 10 ºC order among the most heated point and wooded adjacent points.

Point 3 observed can be seen in Figure 9, which is located in a gated community, divided into apartment blocks. It can be seen that the

warmer area in the cutout image includes a large amount of exposed soil and blocks covered with concrete, which implies an increase in temperature of the local surface, and therefore an increase in air temperature, causing thermal discomfort.

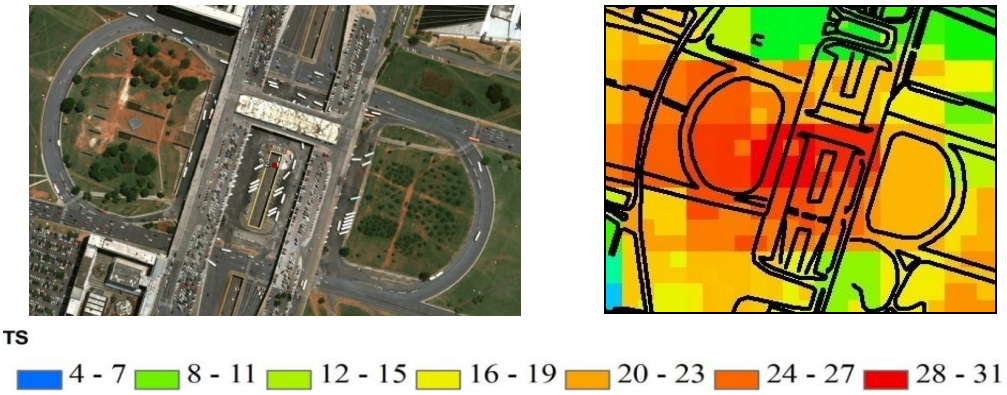

Figure 8 – Spatial distribution of surface temperature between the North and South Wings of the Pilot Plan (Point 2), for the year 2011.

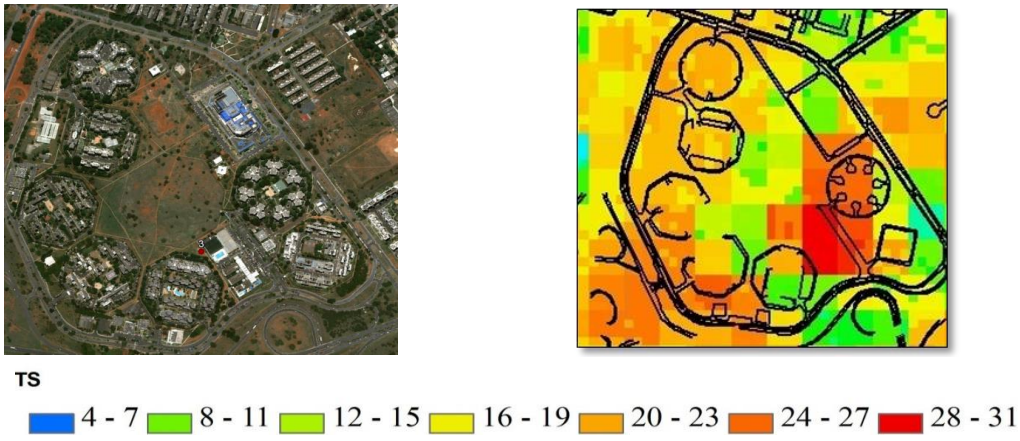

Figure 9 – Spatial distribution of surface temperature in a closed residential condominium (Point 3) , for the year 2011.

The Point 4 selected, located in North Lake, presented a mild statement of formation of the ICU phenomenon, close to the central site, as can be seen in Figure 10, which shows that the replacement of soil cover by asphalt and natural growth cities modify local temperatures.

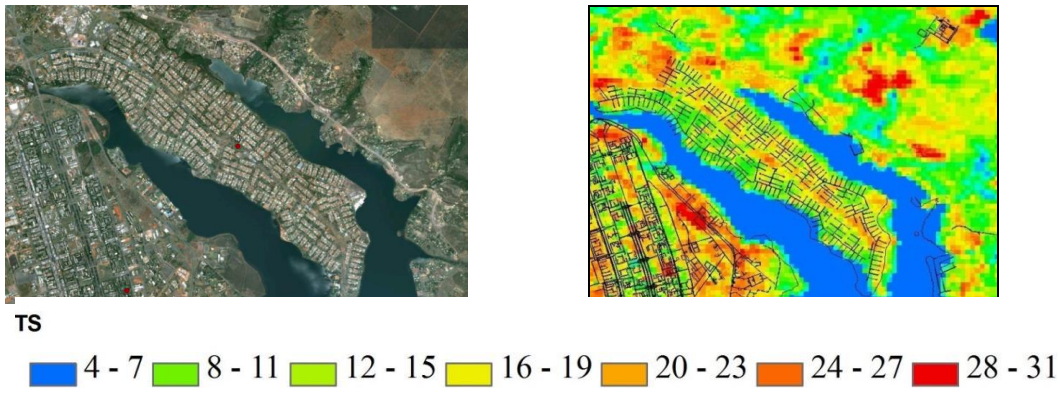

Figure 10 – Spatial distribution of surface temperature of the North Lake area (point 4) for the year 2011.

4. Conclusions

Know the surface temperature of the dynamic over the years can be of great importance for the management of urban space, as these changes may lead to changes in the local microclimate. In this context remote sensing appears as a promising tool of environmental and climate studies.

The results indicate that the expansion of the urban space contributes to a marked increase in surface temperatures over the years, but the pilot plan, it was possible to observe the occurrence of a cooling, which can be derived from the greater presence of vegetation resulting from the implantation of wooded medians, reflecting that in areas planned to climatic criteria, tend to have lower temperatures and respectively a more enjoyable thermal sensation.

In the impermeable areas, with the roads covered in bituminous material and covered buildings mostly with concrete materials and asbestos temperature approached 30 ° C and was verified environments conducive to formation of urban heat islands, for the most heated areas had strong relationship with the material used in roofing, roads, deforestation and waterproofing of recreational areas in general.

Proper management of construction materials in urban areas is of paramount importance, since in addition to the thermal discomfort, high temperatures are likely to cause greater damage to human health, such as increased respiratory diseases, implications in hypertensive and cardiac elderly.

They may also aid in the development and mosquitoes cycle, as is the case of dengue, which increases the possibility of surges within cities, people and can lead to death.

References

Accioly, L.J., Pacheco, A., Costa, T.C.C., Lopes, O.F., Oliveira, A.J., 2002. Relações empíricas entre a estrutura da vegetação e dados do sensor TM/Landsat. Revista Brasileira de Engenharia Agrícola e Ambiental 6, 492-498.

Allen, R.G., Tasumi, M., Trezza, R., Waters, R., 2002. Metric - Mapping evapotranspiration at high resolution and using internalized calibration. Advanced Training and Users Manual. Idaho University, Idaho.

Boegh, E., Soegaard, H., Thomsen, A., 2002. Evaluating evapotranspiration rates and surface conditions using Landsat TM to estimate atmospheric resistance and surface resistance. Remote Sensing of Environment 79, 329-343.

Carlson, T.N., Arthur, S.T., 2000. The impact of land use – land cover changes due to urbanization on surface microclimate and hydrology: a satellite perspective. Global and Plantenaty Change 25, 49-65.

Carneiro, D.P., Genari, H.F., Miyasato, H.H., Martins, R.J., 2007. Ilhas de calor no campus da Unicamp. Revista Ciências do Ambiente 3, 43-48.

Clinton, N., Gong, P., 2013. MODIS detected surface urban heat island and sinks: Global locations and controls. Remote Sensing of Environment 134, 294-304.

Delgado, R.C., Rodrigues, R.A., Faria, A.L.L., Pessoa, C.S., Daher, M., 2012. Uso do sensoriamento remoto na estimativa dos efeitos de ilhas de calor. Revista Brasileira de Ciências Ambientais 25, 69-80.

Essa, W., Verbeiren, B., Van Der Kwast, J., Van De Voorde, T., Batelaan, O., 2011. Evaluation of the DisTrad thermal sharpening methodology for urban areas. International Journal of Applied Earth Observation and Geoinformation 19, 163-172.

Foehlich, J.M., Rauber, C.C., Carpes, R.H., Toebe, M., 2011. Êxodo seletivo, masculinização e envelhecimento da populção rural na região central do RS. Ciência Rural 41, 1674-1680.

Gartland, L., 2010. Ilhas de Calor. Oficina de Textos, São Paulo.

Gutierrez, L.A.R., Souza, G.F., Pereira, G., Paranhos Filho, A.C., Arima, G.A., Barbassa, A.P., 2011. Mapeamento temporal dos índices: área de superfície impermeável e escoamento superficial da área urbanizada de Campo Grande – MS. Caminhos de Geografia 12, 269-288.

Huete, A.R., 1998 A soil adjusted vegetation index – SAVI. Remote Sensing of Environment 25, 295–309.

Huete, A.R., WARRICK, A.W., 1990. Assessment of vegetation and soil water

regimes in partial canopies with optical remotely sensed data. Remote Sensing of Environment 32, 155-167.
IBGE. Instituto Brasileiro de Geografia e Estatística, 2011. Available: http://www.ibge.gov.br. Access: jul., 15, 2011.
Iqbal. M., 1983. An Introduction to Solar Radiation. Academic Press, Canadian.
Koenigsberger, O.H., Ingersoll, T.G., Mayhew, A., Szokolay, S.V., 1980. Manual of Tropical Housing. Nova York.
Lazzarini, M., Marpu, P.R., Ghedira, H., 2013. Temperature-land cover interactions: the inversion of urban heat island phenomenon in desert city areas. Remote Sensing of Environment 130, 136-152.
Lo, C.P., Quattrochi, D.A., 2003. Urban heat island phenomenon and health implications: a remote sensing approach. Photogrammetric Engineering and Remote Sensing 69, 53-1063.
Lombardo, M.A., 1985. Ilha de Calor nas Metrópoles: o exemplo de São Paulo. Hucitec, São Paulo.
Maciel, A., 2002. Projeto bioclimático em Brasília: estudo de caso em edifício de escritórios. Thesis (Master). Santa Catarina, UFSC.
Markham, B.L., Barker, L.L., 1987. Thematic mapper bandpass solar exoatmospherical irradiances. International Journal of Remote Sensing 8, 517- 523.
Menberg, K., Bayer, P., Zosseder, K., Rumohr, S., Blum, P., 2013. Subsurface urban heat islands in German cities. Science of the Total Environment 442, 123-133.
Oke, T.R., 1978. Boundary Layer Climates. London: Methuem & Ltd. A. Halsted Press Book, John Wiley & Sons, New York.
Oke, T.R, 1973. City size and the urban heat island. Atmospheric Environment 7, 769-779.
Patz, J.A., Campbell-Lendrum, D., Olloway, T., Foley, J., 2005. Impact of regional climate change on human health. Nature 438, 310-317.
Pichieri, M., Bonafoni, S., Biondi, R., 2012. Satellite air temperature estimation for monitoring the canopy layer heat island of Milan. Remote Sensing of Environment 127, 130-138.
Ponzonii, F.J., Shimabukuro, Y.E., 2009. Sensoriamento Remoto no Estudo da Vegetação. Parêntese, São José dos Campos.
Serrat, C., Lemonsu, A., Masson, V., Guedalia, D., 2006. Impact of urban heat island on regional atmospheric pollution. Atmospheric Environment 40, 1743-1758.
Stathopoulou, M., Cartalis, C., 2007. Daytime urban heat islands from Landsat ETM+ and Corine land cover data: an application to major cities in Greece. Solar Energy 81, 358-368.
Streutker, D.R., 2003. Sataellite-measured growth of the urban heat island of Houston, Texas. Remote Sensing of Environment 85, 282-289.
Voogt, J.A., Oke, T.R., 2003. Thermal remote sensing of urban climates. Remote Sensing of Environment 86, 370-384.
Yang, X., Hou, Y., Chen, B., 2011. Observed surface warming induced by urbanization in East China. Journal of Geophysical Research 116, 1-12.
Yuan, F.; Bauer, M.E., 2007. Comparison of impervious surface area and normalized difference vegetation index as indicators of surface urban heat island effects in Landsat imagery. Remote Sensing of Environment 106, 375-386.